Cancer Research

Radiotherapy Increases the Permissiveness of Established Mammary Tumors to Rejection by Immunomodulatory Antibodies

Inge Verbrugge[1], Jim Hagekyriakou[3], Leslie L. Sharp[5], Mara Galli[1], Alison West[1], Nicole M. McLaughlin[2], Hélène Duret[2], Hideo Yagita[6], Ricky W. Johnstone[1,4], Mark J. Smyth[2,4], and Nicole M. Haynes[1,4]

Abstract

It is becoming increasingly evident that radiotherapy may benefit from coincident or subsequent immunotherapy. In this study, we examined whether the antitumor effects of radiotherapy, in established triple-negative breast tumors could be enhanced with combinations of clinically relevant monoclonal antibodies (mAb), designed to stimulate immunity [anti-(α)-CD137, α-CD40] or relieve immunosuppression [α-programmed death (PD)-1]. While the concomitant targeting of the costimulatory molecules CD137 and CD40 enhanced the antitumor effects of radiotherapy and promoted the rejection of subcutaneous BALB/c-derived 4T1.2 tumors, this novel combination was noncurative in mice bearing established C57BL/6-derived AT-3 tumors. We identified PD-1 signaling within the AT-3 tumors as a critical limiting factor to the therapeutic efficacy of α-CD137 therapy, alone and in combination with radiotherapy. Strikingly, all mice bearing established orthotopic AT-3 mammary tumors were cured when α-CD137 and α-PD-1 mAbs were combined with single- or low-dose fractionated radiotherapy. $CD8^+$ T cells were essential for curative responses to this combinatorial regime. Interestingly, CD137 expression on tumor-associated $CD8^+$ T cells was largely restricted to a subset that highly expressed PD-1. These $CD137^+PD\text{-}1^{High}$ $CD8^+$ T cells, persisted in irradiated AT-3 tumors, expressed Tim-3, granzyme B and Ki67 and produced IFN-γ *ex vivo* in response to phorbol 12-myristate 13-acetate (PMA) and ionomycin stimulation. Notably, radiotherapy did not deplete, but enriched tumors of functionally active, tumor-specific effector cells. Collectively, these data show that concomitant targeting of immunostimulatory and inhibitory checkpoints with immunomodulatory mAbs can enhance the curative capacity of radiotherapy in established breast malignancy. *Cancer Res; 72(13); 3163–74. ©2012 AACR.*

Introduction

Along with surgery and chemotherapy, radiotherapy is one of the most important anticancer therapies. Indeed, nearly two thirds of all patients with cancer will receive radiotherapy during their course of treatment. Radiotherapy has long been used for its powerful antiproliferative and death-inducing capacities. Recent preclinical and clinical data, however, indicate that immunogenic cell death may also be an important consequence of ionizing radiation (1) and that localized radiotherapy can evoke and/or modulate tumor-associated immune responses (2, 3). Collectively, these findings have set the stage for examining the therapeutic impact of combined radiotherapy and immunotherapy.

Preclinical studies evaluating the combined therapeutic effects of radiotherapy and immunotherapy have employed the use of virus and dendritic cell (DC)-based vaccines (4, 5), Toll-like receptor (TLR) agonists, such as CpG oligodeoxynucleotides (6) and recombinant cytokines (7). In addition, radiotherapy has been trialed in conjunction with monoclonal antibodies (mAb) that target costimulatory molecules such as CD40, CD137, OX40 (CD134), or the checkpoint inhibitor CTLA-4 (8–12). While these studies have shown that single immunomodulatory agents can enhance the antitumor effects of radiotherapy, tumor cures were rare, particularly against poorly immunogenic tumors.

Tumor-induced immune tolerance and immunosuppression (13, 14) may restrict the success of radioimmunotherapeutic approaches. To overcome such immunologic barriers to effectively control established disease, a rational combination of multiple immunomodulatory agents and standard

Authors' Affiliations: [1]Cancer Therapeutics Program, [2]Cancer Immunology Program, Sir Donald and Lady Trescowthick Laboratories and [3]Department of Physical Sciences, Peter MacCallum Cancer Centre, East Melbourne; [4]Sir Peter MacCallum Department of Oncology, University of Melbourne, Parkville, Victoria, Australia; [5]Pfizer Worldwide Research and Development, Oncology Research Unit, San Diego, California; and [6]Department of Immunology, Juntendo University School of Medicine, Tokyo, Japan

Note: Supplementary data for this article are available at Cancer Research Online (http://cancerres.aacrjournals.org/).

R.W. Johnstone, M.J. Smyth, and N.M. Haynes contributed equally as senior authors.

Corresponding Authors: Nicole M. Haynes, Cancer Therapeutics Program & Cancer Immunology Program, Peter MacCallum Cancer Centre, Locked Bag 1, A'Beckett Street, East Melbourne, VIC 8006, Australia. Phone: 613-9656-1752; Fax: 613-9656-1411; E-mail: nicole.haynes@petermac.org; and Inge Verbrugge, Division of Cell Biology II, The Netherlands Cancer Institute, Plesmanlaan 121, 1066 CX Amsterdam, The Netherlands. E-mail: i.verbrugge@nki.nl

doi: 10.1158/0008-5472.CAN-12-0210

anticancer regimens is likely required. Indeed, we and others have shown that combining mAbs targeting CD40, CD1d, and/or CD137, designed to modulate DC and T-cell activity, respectively, are highly effective, particularly in combination with TRAIL-receptor agonists and histone deacetylase inhibitors (HDACi) in eradicating established solid tumors (15–17). However, given the intrinsic resistance of many tumors to TRAIL-receptor agonists and HDACi, as well as the fact that TRAIL-receptor agonists are still in clinical development and the applicability of HDACi is currently largely restricted to hematologic malignancies, the broader application of these combinations is presently limited (18, 19). Blockade of immune checkpoint-inhibitory molecules such as CTLA-4 or programmed death (PD)-1, alone or in combination with anti-(α)-CD137 therapy also increased the therapeutic activity of vaccine approaches and α-erbB2 therapy (20, 21). To date however, the therapeutic benefit of targeting multiple immune stimulatory and/or inhibitory pathways in combination with radiotherapy has not been described.

Here, we show that mAbs to CD137, CD40, and PD-1, which are all in clinical development, combined with single- and low-dose fractionated radiotherapy, induced the rejection of established subcutaneous and orthotopically implanted, triple-negative [estrogen receptor $(ER)^-$, $Her2/neu^-$ and progesterone receptor $(PR)^-$] AT-3 and 4T1.2 mammary tumors. These results are encouraging, given the unmet medical need to treat triple-negative breast cancer in the clinic, as they do not respond to endocrine treatment and other currently available targeted agents. Importantly, we identified the key innate and adaptive immune cells critical to the antitumor effects of radioimmunotherapy. These cells expressed CD137 and/or PD-1 and persisted within the irradiated tumors. This study provides strong validation for combining radiotherapy with immunotherapy and justifies the therapeutic application of both immunostimulatory and checkpoint-inhibitory mAbs as adjuvants to radiotherapy in breast cancer treatment.

Materials and Methods

Mice

Six- to 12-week-old C57BL/6 (B6) and BALB/c mice were obtained from The Walter and Eliza Hall Institute of Medical Research (WEHI) or Animal Resource Centre (Perth, Western Australia). All mice were maintained under specific pathogen-free conditions and used in accordance with institutional guidelines of the Peter MacCallum Cancer Centre.

Cell lines

BALB/c-derived 4T1.2 (22) and B6-derived AT-3 (23) mammary carcinoma cell lines were obtained from Dr Robin Anderson in 2005 and Dr. Trina Stewart in 2007 (Peter MacCallum Cancer Centre, VIC, Australia). Both cell lines were periodically authenticated by morphologic inspection and tested negative for *Mycoplasma* contamination by PCR tests in 2009 to 2010. AT-3 cells, retrovirally transduced to stably express ovalbumin (OVA) were generated as described (24). AT-3 cells were cultured at 37°C, 10% CO_2 in Dulbecco's Modified Eagle's Medium (DMEM), 10% FBS, 0.1 mmol/L nonessential amino acids, 1 mmol/L sodium pyruvate, 2 mmol/L L-glutamine. 4T1.2 cells were cultured at 37°C, 5% CO_2 in RPMI-1640, 10% FBS, 100 μg/mL penicillin/streptomycin, 2 mmol/L L-glutamine.

Cell death and clonogenic assays

For cell death assays, tumor cells were incubated with 10 μmol/L qVD (InSolution Q-VD-OPh; Calbiochem) or corresponding dimethyl sulfoxide (DMSO) concentrations for 30 minutes. Cells were subsequently treated with 0 to 30 Gy ionizing radiation (IR; ^{137}Cs source; at an absorbed dose rate of ~0.6 Gy/min) and harvested 24 to 48 hours post-treatment. Flow cytometry was used to measure (i) cell death by Annexin-V/PI staining and (ii) apoptosis by caspase-3 cleavage as described (25). Clonogenic assays were essentially conducted as described (26). Briefly, cells were plated at increasing densities of up to 8,000 cells/10-cm dish. After adhering (4–6 hours at 37°C), cells were irradiated (0–10 Gy). After 8 to 11 days of incubation under normal culture conditions, cells were stained with 2.5% glutaraldehyde and 0.05% crystal violet for more than 15 minutes at room temperature. Colonies (>40 cells) were counted using an inverted microscope and clonogenicity of untreated cells (0 Gy) was set to 100%.

TUNEL staining

Mice bearing 20 to 25 mm^2 subcutaneous AT-3 tumors were mock-irradiated or treated with 12 Gy radiotherapy. Tumors from control and irradiated mice ($n = 3$) were dissected 16, 24, and 48 hours post-radiotherapy and processed for immunohistochemical analyses [hematoxylin and eosin (H&E) and terminal deoxynucleotidyl transferase–mediated dUTP nick end labeling (TUNEL) staining]. Fixed and paraffin-embedded tissues were randomly sectioned and stained for apoptotic cells using an ApopTag Peroxidase *In Situ* Apoptosis Detection Kit (Chemicon International) as per manufacturers' instructions. Metamorph Imagin Program Series 7.6.3 was used to quantify single, tumor cell–specific TUNEL-positive events (Zeiss Microscope; Carl Zeiss; objective; ×10/0, 30 Plan-Neofluar).

Phenotyping of tumor cells and tumor-infiltrating lymphocytes

Expression of PD-L1 on *in vitro* cultured and explanted tumor cells, before and 12 to 96 hours postradiation treatment (0–30 Gy *in vitro*; 12 Gy *in vivo*) was assessed by flow cytometry as described (27) using biotinylated α-mouse CD274 (PD-L1, BD Pharmingen) mAb and allophycocyanin (APC)-conjugated streptavidin (eBioscience). CD45.2 (eBioscience) staining of explanted tumor samples distinguished leukocytes from tumor cells.

Analysis of tumor-infiltrating leukocytes was conducted before and 16, 36, and 84 hours post-radiotherapy (12 Gy, 5–18 mice/group) for surface expression of CD137 (17B5; eBioscience), PD-1 (J43; eBioscience), CD44 (IM7; BD Pharmingen), CD62L (MEL-14; eBioscience), Tim-3 (RMT3-23; eBioscience), and OVA-tetramer ($K_bOVA_{257-264}$-PE; obtained from S.J. Turner, Department of Microbiology and Immunology, University of Melbourne, Parkville, VIC, Australia).

Intracellular staining for granzyme B (mouse-anti-human granzyme B; BD Bioscience) and Ki67 (mouse-anti-human Ki67; BD Bioscience) was carried out using a Cytofix/Cytoperm, Fixation/Permeabilization Solution Kit according to the manufacturers' instructions (BD Bioscience). Spleens from tumor-bearing mice served as background staining controls. Cell viability was assessed using DAPI (4′,6-diamido-2-phenylindole; Invitrogen) or propidium iodide (PI) and cells were analyzed on a CantoII or LSRII analyzer (BD Biosciences).

Staining for intracellular IFN-γ following phorbol 12-myristate 13-acetate and ionomycin stimulation

Untreated, established (20–25 mm^2) orthotopic AT-3 tumors ($n = 7$) were harvested and processed into single-cell suspensions. Whole-cell preparations were plated at 3×10^5 cells/200 μL DMEM/2% fetal calf serum (FCS) in a 96-well U-bottom plate. Cells were treated with 50 ng/mL phorbol 12-myristate 13-acetate (PMA; Sigma Aldrich) and 1 μg/mL ionomycin (Sigma Aldrich). Control (unstimulated) wells were treated with an equal volume of DMSO. GolgiPlug (1 μg/mL; BD Biosciences) was added to all wells before incubating the cultures for 4 hours at 37°C, 5% CO_2. Staining for intracellular IFN-γ in $CD45.2^+PD\text{-}1^{Low}$ and $PD\text{-}1^{High}$ $CD8^+$ T cells was carried out as described earlier for granzyme B and Ki67 detection and analyzed on a LSRII analyzer.

Therapeutic antibodies and reagents

The rat mAb to mouse CD137 (3H3, IgG2a) was generated in house as described (28) and protein-G purified or purchased from BioXCell. The rat α-mouse CD40 mAb (FGK4.5, IgG2a) was from WEHI. The rat α-mouse PD-1 mAb (RMP1-14; 1gG2a) was prepared as described (29). Depleting antibodies to asialoGM1 [natural killer (NK) cells; Wako Pure Chemical], mouse CD4 (GK1.5), and CD8β (53–5.8; BioXCell) were prepared as described (30). For both therapy and depletion studies, MAC4 mAb was used as the isotype control (28).

Therapy of transplanted tumors

Mice were anesthetized with ketamine (100 mg/kg) and xylazine (10 mg/kg) or isofluorane and injected with 4T1.2 (5×10^4/50 μL PBS) or AT-3 (1×10^6/50 μL PBS) tumor cells subcutaneously on the right hind leg or orthotopically into the fourth mammary fat pad. Tumor size was measured every 2 to 3 days using electronic calipers and represented as tumor area (length × width). Radioimmunotherapy commenced when tumors reached 20 to 25 mm^2. Mice were divided into groups of 4 to 7. Irradiation of subcutaneous tumors was conducted essentially as described (31). Briefly, for irradiation of subcutaneous tumors, mice were inserted into perspex jigs and the tumor bearing leg isolated and restrained for exposure to a single dose of radiation (12 Gy). To minimize exposure of normal tissue to radiotherapy, mice were protected by a 3-mm thick lead shield containing 1.5 cm^2 holes; permitting exposure of the leg to radiotherapy. For irradiation of orthotopic tumors, mice were anesthetized with ketamine/xylazine and positioned under a lead shield containing 0.8 cm^2 exposure holes. Irradiation was delivered using a 6-MeV electron beam at a dose rate of 20 Gy/min (Varian Medical Systems) as a 12 Gy single fraction or in 4 fractions of 4 or 5 Gy at 24-hour intervals. Control mice were placed in radiation jigs (subcutaneous tumors) or anesthetized (orthotopic tumors), but not exposed to radiotherapy.

Immunotherapy consisted of α-CD137 (100 μg) and/or α-CD40 (100 μg), α-PD-1 (100 μg), or MAC4 (100μg) mAbs, administered intraperitoneally on days 0, 4, 8, and 12 relative to radiotherapy. Antibodies depleting $CD4^+$ (100 μg) or $CD8\beta^+$ (50 μg) T cells were administered intraperitoneally on days −1, 0, then every 4 days until day 40, α-asialo GM1 (100 μg) was administered intraperitoneally on days −1, 0, then every 6 days until day 40 relative to radioimmunotherapy.

All radioimmunotherapeutic combinations and treatment regimes were well-tolerated. Mice were sacrificed when tumors reached 100 to 200 mm^2.

Statistics

Statistical differences between groups were analyzed with unpaired Student *t* tests (experiments not involving mice) or Mann–Whitney *U* tests using GraphPad Prism (GraphPad Software).

Results

Ionizing radiation induces cell death in triple-negative mammary tumor cells

In vitro assay systems were initially used to screen the BALB/c-derived 4T1.2 and C57BL/6-derived AT-3 triple-negative mammary tumor lines for their sensitivity to ionizing radiation. Radiation-induced cell death as determined by Annexin-V/PI staining was evident in both cell lines and occurred in a time- and dose-dependent manner (Fig. 1A and B, top). In 4T1.2 cells, radiation-induced cell death was not affected by the pan-caspase inhibitor qVD (Fig. 1A) or overexpression of the antiapoptotic protein Bcl-2 (data not shown). In addition, caspase-3 cleavage was not detected in irradiated 4T1.2 cultures (data not shown); collectively indicating that apoptosis was not the primary mechanism of radiation-induced 4T1.2 cell death. In contrast, caspase-3 cleavage was detected in irradiated AT-3 cultures (Fig. 1B). Overexpression of Bcl-2 (data not shown) or treatment with qVD (Fig. 1B, top) significantly reduced Annexin-V/PI staining, indicating that apoptosis contributed to radiation-induced AT-3 cell death. Despite these mechanistic differences the radiosensitivity of 4T1.2 and AT-3 tumor cells, as determined in long-term clonogenic assays, was comparable (Fig. 1C).

These findings were subsequently confirmed in a neoadjuvant setting of established disease, where a single dose of 12 Gy radiotherapy induced a comparable degree of tumor growth delay in subcutaneous 4T1.2 and AT-3 tumors, without inducing complete regression (Supplementary Fig. S1). TUNEL analysis revealed higher levels of radiotherapy-induced apoptosis in AT-3 than in 4T1.2 tumors *in vivo* [Fig. 1D, (4T1.2)-E (AT-3)]. A modest (<2-fold) but statistically significant increase in the number of apoptotic events, compared with mock treatment was detected 24 hours after radiotherapy in 4T1.2 tumors (Fig. 1D). Whereas in the AT-3 tumors, at 16 hours post-radiotherapy a >10-fold increase in $TUNEL^+$ events, compared

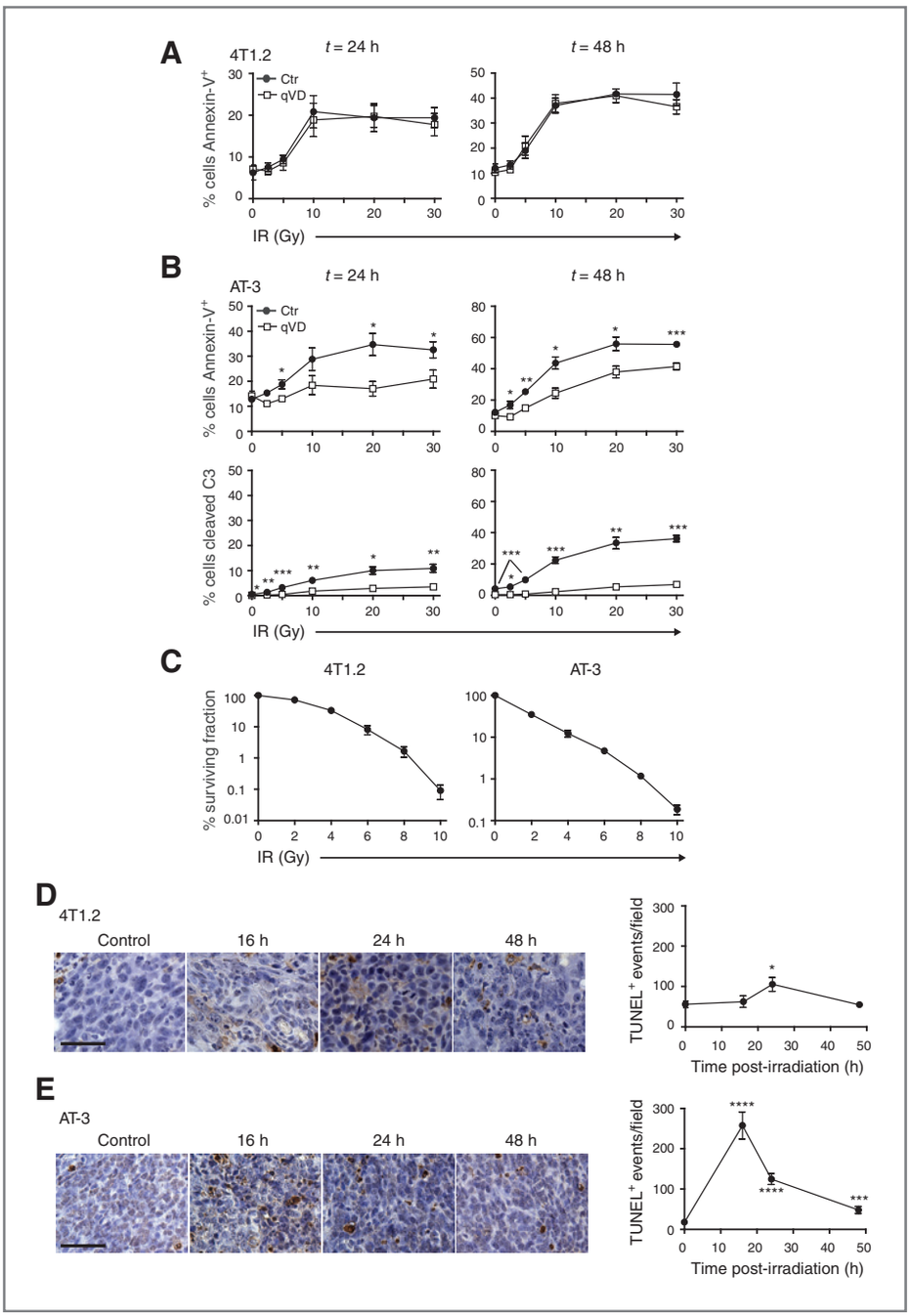

Figure 1. Radiation-induced cell death in mammary tumor cells. Dose–response curves to ionizing radiation (IR) in presence (qVD; squares) or absence (Ctr; circles) of 10 μmol/L qVD are shown for 4T1.2 (A) and AT-3 (B) cell cultures. Annexin-V/PI staining and caspase-3 cleavage were used to quantify cell death and apoptosis. Data points represent mean ± SEM of 3 to 6 independent experiments. *, $P < 0.05$; **, $P < 0.01$; ***, $P < 0.001$, between Ctr and qVD-treated samples. C, clonogenic survival of 4T1.2 and AT-3 cells following treatment with the indicated doses of IR. Data points represent mean ± SEM of 3 independent experiments. D and E, mice bearing subcutaneous 4T1.2 (D) or AT-3 (E) tumors were left untreated or exposed to 12 Gy radiotherapy. At the indicated time points, tumors were harvested and processed for TUNEL analysis (left; Scale bar: 50 μmol/L). Data points represent mean ± SEM of TUNEL$^+$ events per field. *, $P = 0.0132$; ***, $P = 0.0006$; and ****, $P < 0.0001$ at corresponding time points compared with $t = 0$ h.

with mock treatment was observed (Fig. 1E). Importantly, despite differences in the biologic response to radiotherapy, the radioresponsiveness of the 4T1.2 and AT-3 tumors was comparable.

Therapeutic targeting of PD-1 but not CD40 enhanced the curative capacity of radiotherapy/α-CD137 treatment in AT-3 tumors

Previously, we showed that α-CD137/α-CD40 therapy enhanced the antitumor activity of HDACi or α-DR5 therapy in tumor cells that possessed functional apoptotic pathways, suggesting that drug-induced apoptosis engaged antitumor immune responses that could be enhanced with antibody-based immunotherapy (15, 16). On the basis of these results and the ability of radiotherapy to induce apoptosis in AT-3 tumors, we initially analyzed novel radioimmunotherapeutic combinations in AT-3 mammary tumors. We first examined whether α-CD137/α-CD40 therapy could be effectively combined with radiotherapy to control and eradicate subcutaneous AT-3 tumors. Predetermined doses of α-CD40 and/or

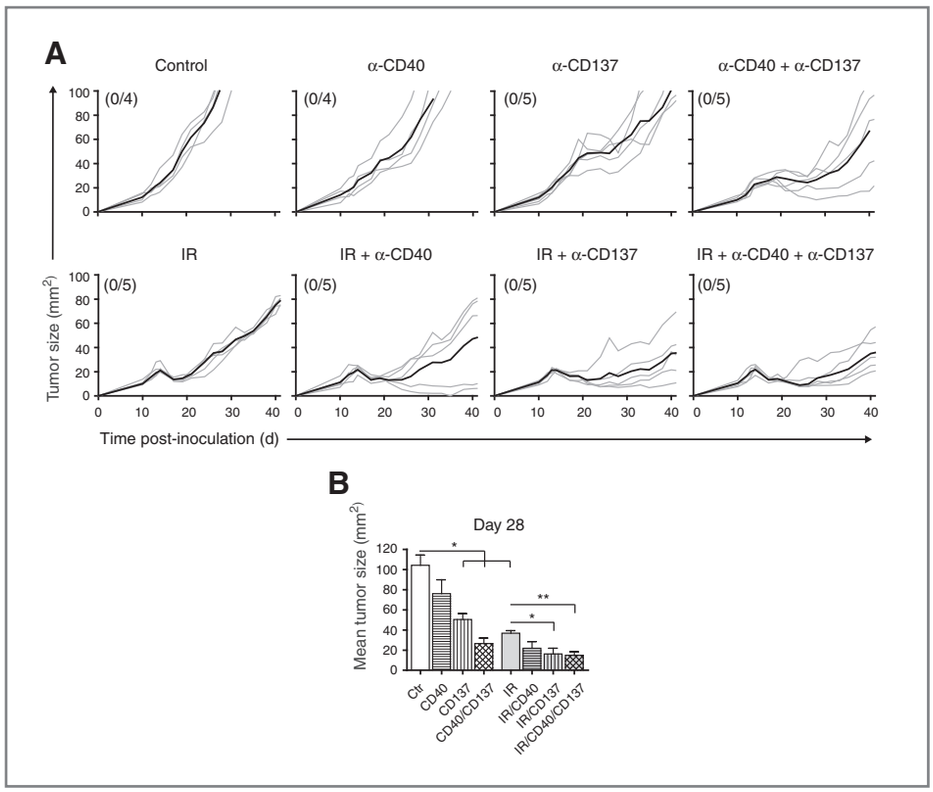

Figure 2. Response of subcutaneous AT-3 tumors to treatment with radiotherapy and α-CD40/α-CD137 mAbs. A, AT-3 tumor-bearing mice were treated with 12 Gy radiotherapy (bottom) or mock-irradiated (top) in combination with α-CD40 and/or α-CD137 mAbs as indicated. Individual tumor growth curves (gray lines) and mean tumor growth (black line) are shown. Numbers in parentheses indicate the fraction of tumor-free mice at 50 days post-tumor inoculation. Results are representative of 2 independent experiments. B, mean tumor sizes in each group from A at day 28 post-tumor inoculation. *, $P < 0.05$; **, $P < 0.01$; and ***, $P < 0.001$.

α-CD137 mAbs were used alone (Fig. 2A, top) or in combination with radiotherapy (12 Gy; Fig. 2A, bottom). Anti-CD137 therapy, alone or in combination with α-CD40 treatment significantly enhanced radiotherapy-induced growth inhibition of AT-3 tumors (Fig. 2A). However, tumors grew out in all mice (Fig. 2A). Although a percentage (40%) of tumor-bearing mice were found to be highly responsive to radiotherapy and α-CD40 treatment (Fig. 2A), α-CD40 therapy did not further enhance the therapeutic response of AT-3 tumors to radiotherapy/α-CD137 treatment (Fig. 2A). Interestingly, however, in established subcutaneous 4T1.2 tumors radiotherapy/α-CD40/α-CD137 therapy was found to be curative in >80% of mice (Supplementary Fig. S2A). The antitumor effects of this triple combination in 4T1.2 tumors were critically dependent on $CD8^+$ T and NK cells (Supplementary Fig. S3A), which expressed CD137 (Supplementary Fig. S3B) and could induce immunologic memory capable of controlling the outgrowth of a secondary tumor challenge (Supplementary Fig. S2). Importantly, these findings show that this novel radioimmunotherapy has the potential to eradicate established, triple-negative mammary tumors.

Given the inability of radiotherapy/α-CD137/α-CD40 treatment to eradicate AT-3 tumors, tumor cell–associated factors that might inhibit the development of an effective antitumor immune response were examined. One candidate was the checkpoint-inhibitory ligand, programmed death-ligand 1 (PD-L1) that has been reported to inhibit T-cell activation on PD-1–expressing T cells, by blocking interleukin (IL)-2 production following TCR stimulation (32). Interestingly, while PD-L1 expression was not detected on *in vitro* cultured AT-3 cells (Fig. 3A, left), explanted AT-3 tumors expressed PD-L1 (Fig. 3A, right), which was unaffected by radiotherapy. On the basis of these observations we examined the therapeutic activity of an antagonistic α-PD-1 mAb in combination with radiotherapy and α-CD137 treatment. While α-PD-1 therapy had no single-agent activity, nor did it enhance the response of AT-3 tumors to radiotherapy (Fig. 3B), α-PD-1 treatment significantly enhanced the responsiveness of AT-3 tumors to radiotherapy/α-CD137 therapy, achieving a rejection rate of up to 40% (Fig. 3B and C). These combined effects were lost in mice depleted of $CD8\beta^+$ T cells and significantly affected by depletion of NK cells (Fig. 3D), but unaffected by depletion of $CD4^+$ T cells (Fig. 3D). Importantly, in mice cured of primary tumors, the outgrowth of secondary AT-3 tumors was significantly impaired, indicating the establishment of immunologic memory (Fig. 3E). Taken together, these data suggest that PD-1 signaling within AT-3 tumors limited the capacity of α-CD137/α-CD40 immunotherapy to support the immunoadjuvant properties of radiotherapy and that inhibition of PD-1 signaling was, therefore, required to optimally promote $CD8^+$ T cell and NK cell function to reject AT-3 tumors.

Rejection of orthotopic AT-3 tumors with radiotherapy/α-CD137/α-PD-1 therapy

We next determined whether α-CD137/α-PD-1 therapy promoted the rejection of irradiated AT-3 tumors in the physiologically relevant tissue microenvironment of the mammary fat pad. Notably, orthotopic AT-3 tumors expressed PD-L1 at levels similar to subcutaneous tumors (data not shown). Combined effects were observed with radiotherapy and

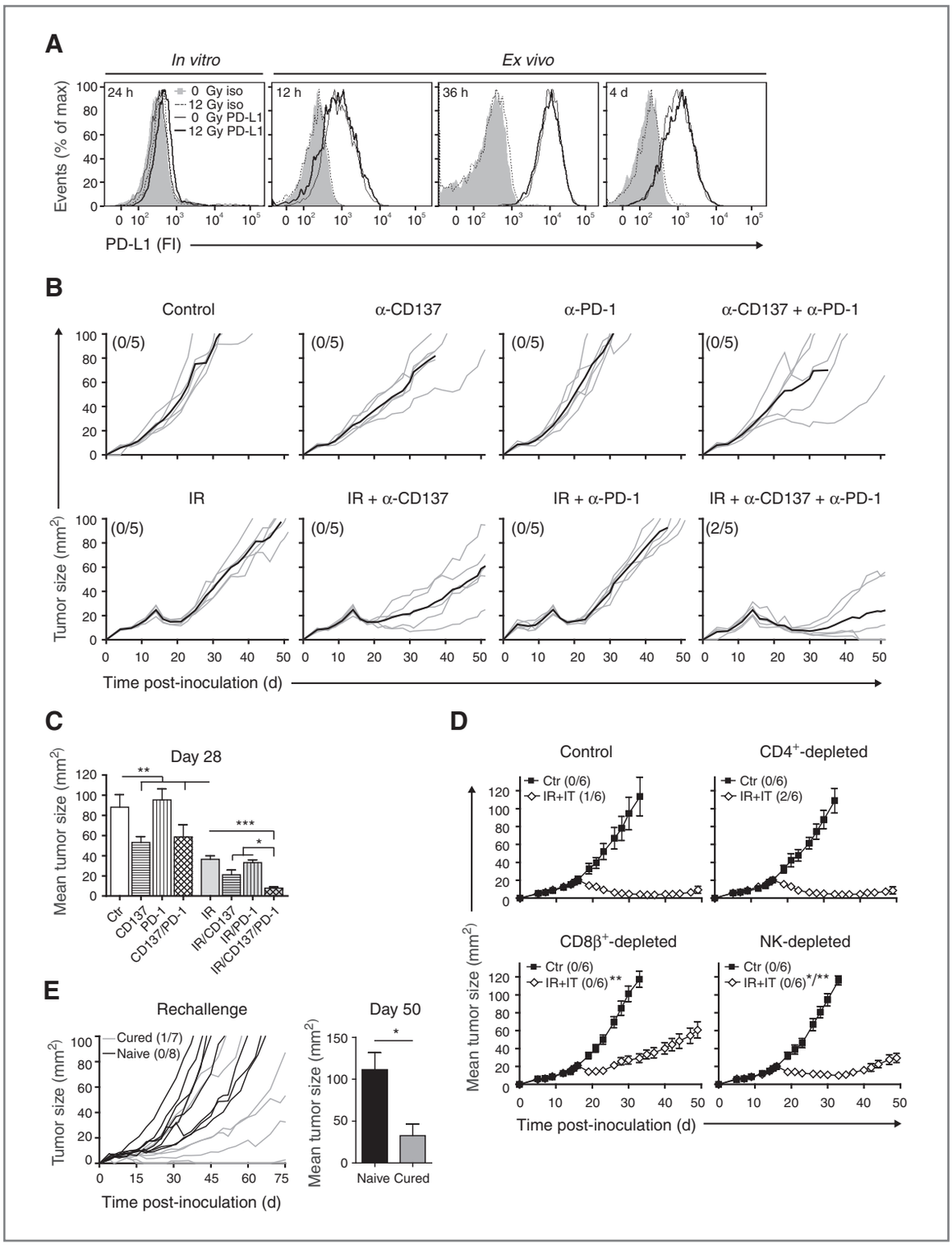

Figure 3. Rejection of established subcutaneous AT-3 tumors with radiotherapy and α-CD137/α-PD-1 mAbs. A, surface expression of PD-L1 on live, *in vitro* cultured AT-3 tumor cells and explanted, live CD45.2$^-$ AT-3 tumor cells, before (narrow line) and at the indicated time points post (bold line) IR. Isotype controls 0 Gy: solid histogram, dashed histogram: 12 Gy. B, AT-3 tumor-bearing mice were treated with 12 Gy radiotherapy (bottom) or mock-irradiated (top) in combination with α-CD137 and/or α-PD-1 mAbs as indicated. Individual tumor growth curves (gray lines) and mean tumor growth (black line) are shown. C, mean tumor sizes in each group in B at day 28 post-tumor inoculation. *, $P < 0.05$; **, $P < 0.01$; and ***, $P < 0.001$. D, AT-3 tumor-bearing mice were treated with cIg (Ctr) or depleting antibodies to CD4, CD8β, or asialoGM1 before mock irradiation and MAC4 (Ctr), or radioimmunotherapy

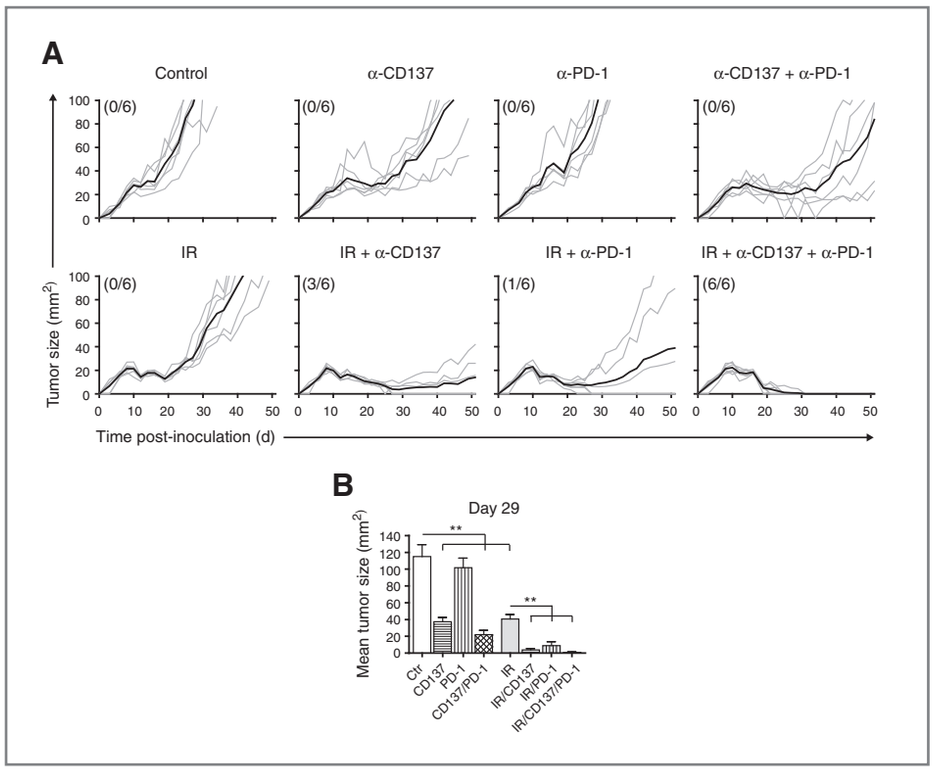

Figure 4. Rejection of established orthotopic AT-3 tumors with radiotherapy and α-CD137/α-PD-1 mAbs. A, mice bearing orthotopic AT-3 tumors were treated with 12 Gy radiotherapy (bottom) or mock-irradiated (top) in combination with α-CD137 and/or α-PD-1 mAbs as indicated. Individual tumor growth curves (gray lines) and mean tumor growth (black line) are shown. Numbers in parentheses indicate the fraction of tumor-free mice 40 days post-tumor inoculation. B, mean tumor sizes in each group from A at day 29 post-tumor inoculation. **, $P < 0.01$.

α-CD137, α-PD-1, and α-CD137/α-PD-1 therapy (Fig. 4A and B). Strikingly, up to a 100% rejection rate was achieved when radiotherapy was combined with both α-CD137 and α-PD-1 mAbs. Consistent with our observations in subcutaneous AT-3 tumors, α-CD137 therapy showed single-agent activity, whereas α-PD-1 treatment did not. However, α-PD-1 treatment prolonged the therapeutic response of orthotopic AT-3 tumors to α-CD137 therapy and significantly enhanced the antitumor effect of radiotherapy in a small percentage of mice (Fig. 4A and B). These results reaffirm the importance of PD-1 as a possible immunotherapeutic target in breast cancer.

Characterization of a persistent CD137$^+$PD-1^{High} CD8$^+$ T-cell subset in irradiated AT-3 tumors

Given the profound therapeutic efficacy of α-CD137/α-PD-1 therapy in irradiated AT-3 tumors, we next examined the AT-3 tumor-associated lymphocytes for expression of CD137 and PD-1. We focused on the characterization of CD8$^+$ T cells as they accounted for more than 40% of the tumor-associated CD45.2$^+$ cells (44.8% ± 3%; 20–25 mm^2 control tumor, $n = 7$) and were the primary mediators of the antitumor activity of radiotherapy/α-CD137/α-PD-1 therapy in subcutaneous AT-3 tumors (Fig. 3D). Interestingly, CD137 expression was only detected on a subset of PD-1^{High}–expressing CD8$^+$ T cells (Fig. 5A). The majority of CD8$^+$ T cells in AT-3 tumors expressed low levels of PD-1 and were negative for CD137 (Fig. 5A). Notably, CD137 and PD-1 expression was also observed on tumor-associated NK and CD4$^+$ T cells (data not shown). Of the PD-1–expressing CD8$^+$ T cells, the PD-1^{Low} subset was most affected by radiotherapy. Indeed the frequency of cells within the PD-1^{Low} population was significantly reduced post-radiotherapy, resulting in a temporary enrichment of the PD-1^{High}CD137$^+$ population of CD8$^+$ T cells (Fig. 5A) and an increased ratio of PD-1^{High} to PD-1^{Low} cells in tumors at 12 hours post-radiotherapy (Fig. 5B).

Further characterization of the tumor-associated PD-1^{High} and PD-1^{Low} subsets revealed that both were CD44$^+$ (Fig. 5C) and CD62L$^-$ (data not shown), two hallmarks of an activated T-cell phenotype. However, expression of the activation marker CD44 was highest on the PD-1^{High} subset, indicative of a more antigen-experienced population (Fig. 5C). In support of this, expression of the immune regulatory molecule T-cell immunoglobulin mucin (Tim)-3, which has been linked to TCR engagement and proliferation (33) was also found to be tightly

Figure 3. *Continued*. [radiotherapy/α-CD137/α-PD-1 mAbs, (IR + IT)]. Results represent mean tumor growth ± SEM. Differences between growth curves in the radioimmunotherapy-treated groups are indicated: control versus CD8 T-cell depletion (from day 23 post-tumor inoculation); **, $P < 0.01$; control versus NK cell depletion (days 23, 26, 33, 37, and 49); *, $P < 0.05$; (days 30, 35, 40, 42, 44, 46); **, $P < 0.01$. E, left, tumor-free, IR/α-CD137/α-PD-1–treated mice were rechallenged with 10^6 AT-3 cells (gray lines) >80 days after primary AT-3 tumor clearance. Growth of secondary subcutaneous tumor inocula were assessed against primary AT-3 tumor growth in naive B6 mice (black lines). Right, mean tumor sizes in naive and cured mice at day 50 post-tumor inoculation. *, $P = 0.013$. Results are pooled data from 2 independent experiments. B, D, and E, numbers in parentheses indicate the fraction of tumor-free mice 40 days post-tumor inoculation.

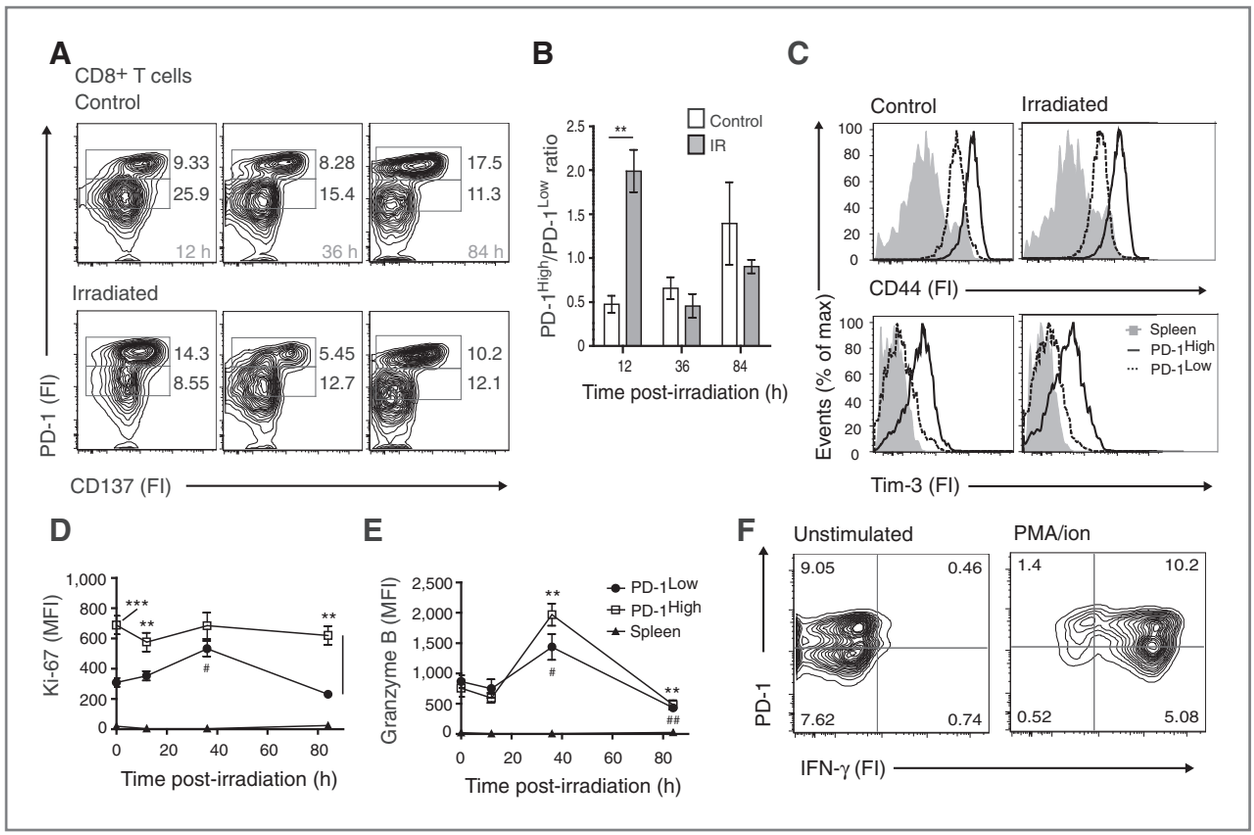

Figure 5. Characterization of the immune cell subsets contributing to the rejection of orthotopic AT-3 tumors. A, mice bearing orthotopic AT-3 tumors were treated with 12 Gy radiotherapy or mock-irradiated. At the indicated time points, CD45.2$^+$CD8$^+$ tumor-infiltrating T cells were analyzed for CD137 and PD-1 expression. The contour plots represent a concatenated analysis of CD137 and PD-1 expression for all mice within each group ($n = 6$–18). The concatenated frequency of CD45.2$^+$PD-1^{Low} and PD-1^{High}CD8$^+$ T cells is shown for each time point in each group. B, ratio of CD45.2$^+$CD8$^+$PD-1^{High}/CD45.2$^+$CD8$^+$PD-1^{Low} cells in the control and irradiated tumors analyzed in A at all indicated time points. **, $P < 0.01$ between control and IR groups at 12 hours. Results are representative of 2 independent experiments. C, surface expression of CD44 (top) and Tim-3 (bottom) on gated tumor-associated CD45.2$^+$, CD62L$^-$, PD-1^{Low}, and PD-1^{High} CD8$^+$ T-cells from control (mock-irradiated) and irradiated AT-3 tumors, 12 hours post-treatment. Spleen (Sp): solid histogram, PD-1^{High} subset: solid line histogram, PD-1^{Low} subset: dashed histogram. Concatenated analysis ($n = 6$). D and E, quantification of intracellular Ki67 (D) and granzyme B (E) expression in tumor-associated PD-1^{High} and PD-1^{Low}–expressing CD8$^+$ T-cell subsets at 12, 36, and 84 hours after 12 Gy radiotherapy ($n = 6$–18/group) or concatenated analysis of mock treatment from all these time points ($t = 0$ hour; $n = 18$). In D, **, $P < 0.01$; ***, $P < 0.001$ between PD-1^{High} and PD-1^{Low} subsets at the indicated time points; #, $P < 0.05$ at 36 hours after radiotherapy for the PD-1^{Low} T-cell subset compared with $t = 0$ hour. In (E), **, $P < 0.01$ at corresponding time points compared with $t = 0$ hour for the PD-1^{High} T-cell subset and #, $P < 0.05$; ##, $P < 0.01$ at corresponding time points compared with $t = 0$ hour for the PD-1^{Low} T-cell subset compared with $t = 0$ hour. F, flow cytometric analysis of intracellular IFN-γ in CD45.2$^+$PD-1^{Low} and PD-1^{High} CD8$^+$ T cells in unstimulated and PMA/ionomycin-stimulated cultures from untreated, established AT-3 tumors. Contour plots represent concatenated analysis of intracellular IFN-γ in the PD-1^{Low} and PD-1^{High}CD45.2$^+$ gated CD8$^+$ T cells for all mice ($n = 7$). Frequency of CD45.2$^+$ cells is shown for each quadrant.

associated with this PD-1^{High} subset (Fig. 5C). Notably, radiotherapy did not alter the expression status of either of these molecules on the PD-1^{High} and PD-1^{Low} CD8$^+$ T-cell subsets (Fig. 5C). Assessment of their proliferative status by Ki67 staining showed that both PD-1^{High} and PD-1^{Low}–expressing cell populations were actively proliferating (Fig. 5D). Ki67 staining was highest in the PD-1^{High} subset and was unaffected by radiotherapy. In contrast, Ki67 expression within the PD-1^{Low}CD8$^+$ T-cell population increased at 36 hours post-radiotherapy. This observation may account for the normalization of the PD-1^{High}/PD-1^{Low} CD8$^+$ T-cell ratio seen between 12 and 36 hours post-radiotherapy (Fig. 5B). Despite these differences, both the PD-1^{High} and PD-1^{Low}CD8$^+$ T-cell subsets possessed similar levels of granzyme B, which was increased at 36 hours post-radiotherapy (Fig. 5E). Further to this, the PD-1^{High} and PD-1^{Low} CD8$^+$ T-cell subsets were equally capable of producing IFN-γ in response to PMA and ionomycin (Fig. 5F), suggesting that both were functionally active *ex vivo*. Importantly, these functionally responsive populations of CD137$^+$CD8$^+$ T cells persisted post-radiotherapy, highlighting the fact that radiotherapy does not deplete, but can enrich tumors for critical effector cells, capable of driving immune responses to dying tumor cells.

Tumor specificity is associated with PD-1^{High}CD137$^+$CD8$^+$ T cells

To investigate whether radiotherapy enriched AT-3 tumors for tumor-reactive CD8$^+$ T cells, we examined the

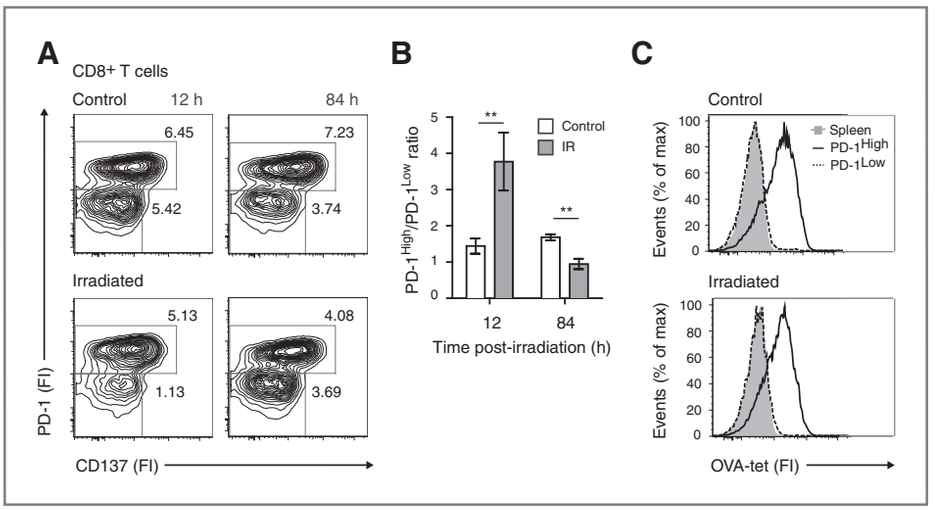

Figure 6. Antigen specificity of CD137$^+$PD-1^{High} and PD-1^{low} CD8$^+$ T cells. A, mice bearing orthotopic OVA-expressing AT-3 tumors were treated with radiotherapy. CD45.2$^+$CD8$^+$ tumor-infiltrating T cells in explanted AT-3 tumors were analyzed and contour plots generated as described for Fig. 5A ($n = 6$–18 mice/group). The concatenated frequency of CD45.2$^+$PD-1^{Low} and PD-1^{High} CD8$^+$ T cells is shown for each time point in each group. B, ratio of CD45.2$^+$CD8$^+$PD-1^{High}/CD45.2$^+$CD8$^+$PD-1^{Low} cells in control and irradiated tumors analyzed in A at all indicated time points. **, $P < 0.01$. C, flow cytometric plots showing OVA tetramer staining within PD-1^{High} and PD-1^{Low}CD8$^+$ T-cell populations from mice analyzed in A. Spleen from tumor-bearing mice served as background staining control.

tumor specificity of the PD-1^{High} and PD-1^{Low} CD8$^+$ T-cell subsets in explanted OVA-expressing orthotopic AT-3 tumors by OVA-tetramer staining. Similar to what was observed in the parental AT-3 tumors, CD137 expression was restricted to the PD-1^{High}CD8$^+$ T-cell subset (Fig. 6A), which was enriched for at 12 hours following radiotherapy (Fig. 6A and B). Importantly, only cells within the PD-1^{High}-CD137$^+$CD8$^+$ T-cell population were OVA-tetramer reactive and thus tumor antigen-specific (Fig. 6C), which indicates that radiotherapy enriches the tumor microenvironment for tumor-specific CD8$^+$ T cells.

Fractionated radiotherapy in combination with immunotherapy induces regression of orthotopic mammary tumors

Although our data so far highlight the therapeutic potential of radioimmunotherapy for the treatment of breast cancer, in the clinic, patients typically receive a series of low-dose fractionated treatments of radiotherapy to limit normal tissue toxicity. We therefore examined whether concomitant targeting of CD137 and PD-1 could reject established orthotopic AT-3 tumors treated with fractionated radiotherapy. Certainly this approach seemed viable given that single-dose 12 Gy radiotherapy did not deplete the AT-3 tumors of CD137$^+$CD8$^+$ T cells. On the basis of the clonogenic survival curve in Fig. 1C, mice were treated with 4 fractions of 4 Gy, achieving a dose close to 12 Gy, or 4 fractions of 5 Gy. Anti-CD137/α-PD-1 therapy in combination with either 4 × 4 Gy or 4 × 5 Gy was more effective in controlling tumor outgrowth than either treatment alone; achieving rejection rates of 40% and 80%, respectively (Fig. 7A and B). The finding that antibody-based immunotherapy enhanced the antitumor response to low-dose fractionated radiotherapy shows the clinical potential of this radioimmunotherapeutic approach for treating established breast cancer.

Discussion

To our knowledge, this is the first preclinical study to examine the therapeutic impact of combining multiple stimulatory and/or inhibitory mAbs with radiotherapy and the cellular mechanisms underlying these responses in established breast cancer. We show in two distinct models of triple-negative mammary cancer that unique combinations of radioimmunotherapy are capable of curing mice of established disease. Radioimmunotherapy was well-tolerated and effective when used in a clinically relevant fractionated radiotherapy regime against orthotopically implanted tumors. The profound therapeutic efficacy of radiotherapy in combination with α-CD137/α-PD-1 therapy in established AT-3 tumors is likely linked to the capacity of radiotherapy to enrich the tumor microenvironment of critical tumor-reactive CD8$^+$ T cells that coexpress CD137 and PD-1.

The checkpoint-inhibitory receptor PD-1 plays an important role in the regulation of immune responses and maintenance of peripheral immune tolerance (34). However, in the context of tumor immunity, the inhibitory actions of PD-1 can be deleterious to the development of robust antitumor immune responses (reviewed in ref. 35). While antibody-mediated blockade of PD-1 signaling had minimal impact on the growth of irradiated AT-3 tumors, it significantly enhanced the curative capacity of radiotherapy/α-CD137 therapy in this model; highlighting PD-1 signaling as a potential limiting factor to the therapeutic success of radioimmunotherapy. Interestingly, α-CD137/α-PD-1 therapy was equally as effective as radiotherapy in suppressing orthotopic tumor growth, highlighting the

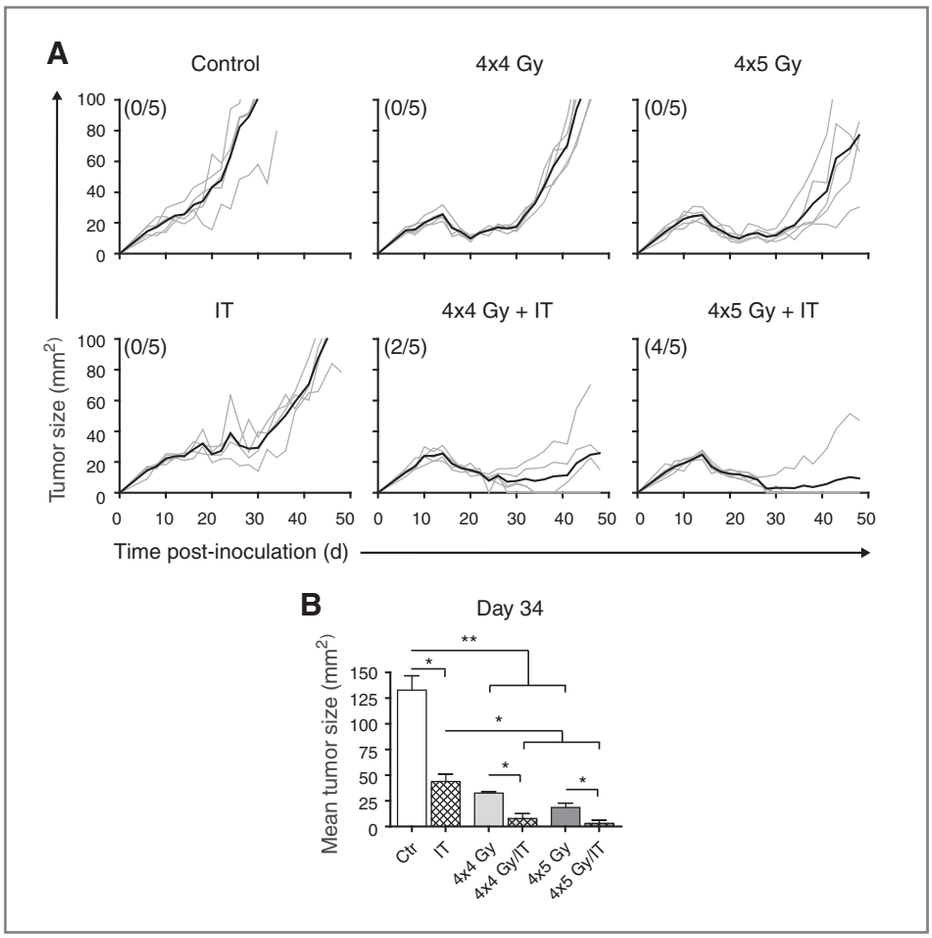

Figure 7. Fractionated radiotherapy in combination with immunotherapy induces regression of orthotopic AT-3 tumors. A, mice bearing orthotopic AT-3 tumors were treated with 4 fractions of 4 or 5 Gy radiotherapy (middle and right) or mock-irradiated (left) in combination with α-CD137/α-PD-1 mAbs (bottom) or cIg (top). Individual tumor growth curves (gray lines) and mean tumor growth (black line) are shown. Numbers in parentheses indicate the fraction of tumor-free mice 40 days posttumor inoculation. B, mean tumor sizes in each group in Fig. 6A at day 34 posttumor inoculation. **, $P < 0.01$.

capacity of α-CD137/α-PD-1 mAbs to re-engage the antitumor activity of tumor-associated lymphocytes. Consistent with this, CD137 expression on AT-3 tumor-associated $CD8^+$ T cells, which were critical for the antitumor activity of radiotherapy/α-CD137/α-PD-1, was restricted to a PD-1^{High}–expressing subset. These $CD137^+$PD-$1^{High}CD8^+$ T cells also expressed the immune regulatory molecule Tim-3. The coexpression of PD-1 and Tim-3 has been associated with an exhausted T-cell phenotype (36). However, the similarities between the PD-$1^{High}Tim3^+$ and PD-$1^{Low}Tim3^-$ $CD8^+$ T-cell populations in terms of IFN-γ production, proliferative status and cytolytic potential, suggests that the PD-$1^{High}CD8^+$ T-cell subset is not an exhausted population but comprises of terminally differentiated, antigen-responsive cells. Interestingly, in mice bearing OVA-expressing AT-3 tumors, all tumor-associated OVA-tetramer$^+CD8^+$ T cells coexpressed CD137 and PD-1. While endogenous AT-3 antigens and antigen-specific $CD8^+$ T cells have yet to be characterized, these results strongly suggest that tumor-specific $CD8^+$ T cells reside within the tumor-associated $CD137^+$PD-1^{High} subset and thus could be the primary targets of α-CD137/α-PD-1 therapy.

The temporary enrichment of PD-1^{High} $CD8^+$ T cells in irradiated AT-3 tumors and concomitant loss of PD-1^{Low}–expressing $CD8^+$ T cells is intriguing and further favors the PD-1^{High}–expressing cells as immunotherapeutic targets of α-PD-1 therapy. The reasons for the differential responsiveness of PD-1^{High}- and PD-1^{Low}–expressing $CD8^+$ T-cell subsets to radiotherapy are still unclear. However, it is tempting to speculate, based on their $CD44^{High}CD62L^-$ phenotype that the antigen-experienced PD-1^{High} subset comprises of more committed or terminally differentiated tumor-specific T cells and thus are more radioresistant. Indeed, studies have reported the acquisition of radioresistance by T cells upon encountering tumor antigen *in vivo* (37). Furthermore, within the PD-$1^{Low}CD8^+$ T-cell pool, a population of suppressor T cells may exist, which are characteristically more radiosensitive than other T cells (38, 39). Alternatively, radiotherapy may promote a more rapid and/or preferential recruitment of antigen-experienced PD-1^{High} T cells into the tumor microenvironment than "nonspecific" or newly engaged tumor-reactive $CD8^+$ T cells.

In 4T1.2 tumors, which in contrast to the AT-3 model, supported a necrotic core (Supplementary Fig. S4) and died in response to radiotherapy in a nonapoptotic manner, α-PD-1 therapy alone was sufficient to reject irradiated tumors (Supplementary Fig. S5). These data suggest that the inflammatory nature of the tumor microenvironment can impact upon the potency of radioimmunotherapy. In line with this, while

radiotherapy/α-CD137/α-CD40 therapy was noncurative in established subcutaneous AT-3 tumors, this novel combination increased the survival rate achieved with radiotherapy alone by greater than 70% in 4T1.2 tumors. These results are significant given the high metastatic potential of these tumors (40) and show the immunogenic nature of nonapoptotic radiation-induced cell death (reviewed in refs. 41, 42).

Given the efficacy of α-CD137 therapy in irradiated AT-3 and 4T1.2 tumors, we predicted that antibody-based targeting of other costimulatory receptors might mediate similar therapeutic effects. The CD137 family member OX40 has been reported to enhance $CD8^+$ T-cell–dependent antitumor effects of radiotherapy in highly immunogenic OVA-expressing Lewis lung carcinoma and MCA205 sarcoma (8, 43) and was therefore of particular interest. Surprisingly however, α-OX40 therapy did not enhance the therapeutic efficacy of radiotherapy in 4T1.2 (Supplementary Fig. S6A) and AT-3 tumors (Supplementary Fig. S6B). The reasons for the lack of α-OX40 activity in these models remain unresolved; however α-CD137 therapy can also directly alter expression of adhesion molecules on tumor endothelial tissue, which can in turn promote infiltration of activated T cells (44). It is therefore possible that other factors before or post-radiotherapy, account for the different levels of α-CD137 and α-OX40 mAb activity in 4T1.2 and AT-3 tumors.

In summary, we found that single-dose and fractionated radiotherapy can be safely and effectively combined with multiple immunostimulatory and/or -inhibitory mAbs to cure mice of established triple-negative mammary tumors. Importantly, functionally responsive, tumor-reactive lymphocytes, expressing clinically viable immunologic targets such as CD137 and/or PD-1 persisted within irradiated tumors. Collectively, these results provide strong validation for combining radiotherapy with multiple immunostimulatory and inhibitory signaling pathways in patients with breast cancer treated with neoadjuvant radiotherapy. We predict that cancers of other tissue origins, in which radiotherapy is used as the primary course of treatment, will also be responsive to such therapeutic strategies.

Disclosure of Potential Conflicts of Interest

During the preparation of the manuscript, L.L. Sharp was an employee of Pfizer and has ownership interest (including patents) for the same. No potential conflicts of interest were disclosed by other authors.

Authors' Contributions

Conception and design: I. Verbrugge, L.L. Sharp, R.W. Johnstone, M.J. Smyth, N. M. Haynes

Development of methodology: A.C. West, H. Yagita, N.M. Haynes

Acquisition of data (provided animals, acquired and managed patients, provided facilities, etc.): I. Verbrugge, J. Hagekyriakou, M. Galli, A.C. West, N.M. Haynes

Analysis and interpretation of data (e.g., statistical analysis, biostatistics, computational analysis): I. Verbrugge, M. Galli, A.C. West, M.J. Smyth, N.M. Haynes

Writing, review, and/or revision of the manuscript: I. Verbrugge, J. Hagekyriakou, L.L. Sharp, H. Yagita, R.W. Johnstone, M.J. Smyth, N.M. Haynes

Administrative, technical, or material support (i.e., reporting or organizing data, constructing databases): J. Hagekyriakou, N.M. McLaughlin, H. Duret, H. Yagita, M.J. Smyth

Study supervision: L.L. Sharp, R.W. Johnstone, M.J. Smyth, N.M. Haynes

Acknowledgments

The authors thank Susan Jackson and Rachel Walker for technical assistance.

Grant Support

This work was financially supported by the Dutch Cancer Society to I. Verbrugge (NKI2009-4446); National Health and Medical Research Council of Australia (NHMRC) program grants, Susan G. Komen Breast Cancer Foundation, Victorian Cancer Agency (to M.J Smyth and R.W Johnstone); Victorian Breast Cancer Research Consortium (to R.W. Johnstone, M.J. Smyth, and N.M. Haynes); Leukemia Foundation of Australia, Australian Rotary Health Foundation (to R.W. Johnstone); an NHMRC Fellowship (to M.J. Smyth); Pfizer, Cancer Australia and a Cure Cancer Australia grant (to N.M. Haynes).

The costs of publication of this article were defrayed in part by the payment of page charges. This article must therefore be hereby marked *advertisement* in accordance with 18 U.S.C. Section 1734 solely to indicate this fact.

Received January 25, 2012; revised April 4, 2012; accepted April 22, 2012; published OnlineFirst May 8, 2012.

References

1. Apetoh L, Ghiringhelli F, Tesniere A, Criollo A, Ortiz C, Lidereau R, et al. The interaction between HMGB1 and TLR4 dictates the outcome of anticancer chemotherapy and radiotherapy. Immunol Rev 2007; 220:47–59.
2. Reits EA, Hodge JW, Herberts CA, Groothuis TA, Chakraborty M, Wansley EK, et al. Radiation modulates the peptide repertoire, enhances MHC class I expression, and induces successful antitumor immunotherapy. J Exp Med 2006;203:1259–71.
3. Formenti SC, Demaria S. Systemic effects of local radiotherapy. Lancet Oncol 2009;10:718–26.
4. Chakraborty M, Abrams SI, Coleman CN, Camphausen K, Schlom J, Hodge JW. External beam radiation of tumors alters phenotype of tumor cells to render them susceptible to vaccine-mediated T-cell killing. Cancer Res 2004;64:4328–37.
5. Gulley JL, Arlen PM, Bastian A, Morin S, Marte J, Beetham P, et al. Combining a recombinant cancer vaccine with standard definitive radiotherapy in patients with localized prostate cancer. Clin Cancer Res 2005;11:3353–62.
6. Mason KA, Ariga H, Neal R, Valdecanas D, Hunter N, Krieg AM, et al. Targeting toll-like receptor 9 with CpG oligodeoxynucleotides enhances tumor response to fractionated radiotherapy. Clin Cancer Res 2005;11:361–9.
7. Lee J, Moran JP, Fenton BM, Koch CJ, Frelinger JG, Keng PC, et al. Alteration of tumour response to radiation by interleukin-2 gene transfer. Br J Cancer 2000;82:937–44.
8. Yokouchi H, Yamazaki K, Chamoto K, Kikuchi E, Shinagawa N, Oizumi S, et al. Anti-OX40 monoclonal antibody therapy in combination with radiotherapy results in therapeutic antitumor immunity to murine lung cancer. Cancer Sci 2008;99:361–7.
9. Shi W, Siemann DW. Augmented antitumor effects of radiation therapy by 4-1BB antibody (BMS-469492) treatment. Anticancer Res 2006; 26:3445–53.
10. Dewan MZ, Galloway AE, Kawashima N, Dewyngaert JK, Babb JS, Formenti SC, et al. Fractionated but not single-dose radiotherapy induces an immune-mediated abscopal effect when combined with anti-CTLA-4 antibody. Clin Cancer Res 2009;15:5379–88.
11. Demaria S, Kawashima N, Yang AM, Devitt ML, Babb JS, Allison JP, et al. Immune-mediated inhibition of metastases after treatment with local radiation and CTLA-4 blockade in a mouse model of breast cancer. Clin Cancer Res 2005;11:728–34.
12. Honeychurch J, Glennie MJ, Johnson PW, Illidge TM. Anti-CD40 monoclonal antibody therapy in combination with irradiation results in a CD8 T-cell-dependent immunity to B-cell lymphoma. Blood 2003;102:1449–57.

13. Shiao SL, Coussens LM. The tumor-immune microenvironment and response to radiation therapy. J Mammary Gland Biol Neoplasia 2010;15:411–21.
14. Stewart TJ, Abrams SI. How tumours escape mass destruction. Oncogene 2008;27:5894–903.
15. Uno T, Takeda K, Kojima Y, Yoshizawa H, Akiba H, Mittler RS, et al. Eradication of established tumors in mice by a combination antibody-based therapy. Nat Med 2006;12:693–8.
16. Christiansen AJ, West A, Banks KM, Haynes NM, Teng MW, Smyth MJ, et al. Eradication of solid tumors using histone deacetylase inhibitors combined with immune-stimulating antibodies. Proc Natl Acad Sci U S A 2011;108:4141–6.
17. Teng MW, Sharkey J, McLaughlin NM, Exley MA, Smyth MJ. CD1d-based combination therapy eradicates established tumors in mice. J Immunol 2009;183:1911–20.
18. Bellail AC, Qi L, Mulligan P, Chhabra V, Hao C. TRAIL agonists on clinical trials for cancer therapy: the promises and the challenges. Rev Recent Clin Trials 2009;4:34–41.
19. Verbrugge I, Johnstone RW, Bots M. Promises and challenges of anticancer drugs that target the epigenome. Epigenomics 2011;3: 547–65.
20. Curran MA, Montalvo W, Yagita H, Allison JP. PD-1 and CTLA-4 combination blockade expands infiltrating T cells and reduces regulatory T and myeloid cells within B16 melanoma tumors. Proc Natl Acad Sci U S A 2010;107:4275–80.
21. Stagg J, Loi S, Divisekera U, Ngiow SF, Duret H, Yagita H, et al. Anti-ErbB-2 mAb therapy requires type I and II interferons and synergizes with anti-PD-1 or anti-CD137 mAb therapy. Proc Natl Acad Sci U S A 2011;108:7142–7.
22. Tester AM, Ruangpanit N, Anderson RL, Thompson EW. MMP-9 secretion and MMP-2 activation distinguish invasive and metastatic sublines of a mouse mammary carcinoma system showing epithelial-mesenchymal transition traits. Clin Exp Metastasis 2000;18:553–60.
23. Stewart TJ, Abrams SI. Altered immune function during long-term host-tumor interactions can be modulated to retard autochthonous neoplastic growth. J Immunol 2007;179:2851–9.
24. Mattarollo SR, Loi S, Duret H, Ma Y, Zitvogel L, Smyth MJ. Pivotal role of innate and adaptive immunity in anthracycline chemotherapy of established tumors. Cancer Res 2011;71:4809–20.
25. Verbrugge I, de Vries E, Tait SW, Wissink EH, Walczak H, Verheij M, et al. Ionizing radiation modulates the TRAIL death-inducing signaling complex, allowing bypass of the mitochondrial apoptosis pathway. Oncogene 2008;27:574–84.
26. Verbrugge I, Wissink EH, Rooswinkel RW, Jongsma J, Beltraminelli N, Dupuis M, et al. Combining radiotherapy with APO010 in cancer treatment. Clin Cancer Res 2009;15:2031–8.
27. Haynes NM, Hawkins ED, Li M, McLaughlin NM, Hammerling GJ, Schwendener R, et al. CD11c+ dendritic cells and B cells contribute to the tumoricidal activity of anti-DR5 antibody therapy in established tumors. J Immunol 2010;185:532–41.
28. Takeda K, Yamaguchi N, Akiba H, Kojima Y, Hayakawa Y, Tanner JE, et al. Induction of tumor-specific T cell immunity by anti-DR5 antibody therapy. J Exp Med 2004;199:437–48.
29. Yamazaki T, Akiba H, Koyanagi A, Azuma M, Yagita H, Okumura K. Blockade of B7-H1 on macrophages suppresses CD4+ T cell proliferation by augmenting IFN-gamma-induced nitric oxide production. J Immunol 2005;175:1586–92.
30. Frew AJ, Lindemann RK, Martin BP, Clarke CJ, Sharkey J, Anthony DA, et al. Combination therapy of established cancer using a histone deacetylase inhibitor and a TRAIL receptor agonist. Proc Natl Acad Sci U S A 2008;105:11317–22.
31. Solomon B, Hagekyriakou J, Trivett MK, Stacker SA, McArthur GA, Cullinane C. EGFR blockade with ZD1839 ("Iressa") potentiates the antitumor effects of single and multiple fractions of ionizing radiation in human A431 squamous cell carcinoma. Epidermal growth factor receptor. Int J Radiat Oncol Biol Phys 2003;55:713–23.
32. Riley JL. PD-1 signaling in primary T cells. Immunol Rev 2009;229: 114–25.
33. Mujib S, Jones RB, Lo C, Aidarus N, Clayton K, Sakhdari A, et al. Antigen-independent induction of Tim-3 expression on human T cells by the common gamma-chain cytokines IL-2, IL-7, IL-15, and IL-21 is associated with proliferation and is dependent on the phosphoinositide 3-kinase pathway. J Immunol 2012;188:3745–56.
34. Okazaki T, Honjo T. PD-1 and PD-1 ligands: from discovery to clinical application. Int Immunol 2007;19:813–24.
35. Weber J. Immune checkpoint proteins: a new therapeutic paradigm for cancer–preclinical background: CTLA-4 and PD-1 blockade. Semin Oncol 2010;37:430–9.
36. Jones RB, Ndhlovu LC, Barbour JD, Sheth PM, Jha AR, Long BR, et al. Tim-3 expression defines a novel population of dysfunctional T cells with highly elevated frequencies in progressive HIV-1 infection. J Exp Med 2008;205:2763–79.
37. Dunn PL, North RJ. Selective radiation resistance of immunologically induced T cells as the basis for irradiation-induced T-cell-mediated regression of immunogenic tumor. J Leukoc Biol 1991;49: 388–96.
38. Schatten S, Granstein RD, Drebin JA, Greene MI. Suppressor T cells and the immune response to tumors. Crit Rev Immunol 1984;4: 335–79.
39. Enker WE, Jacobitz JL. *In vivo* splenic irradiation eradicates suppressor T-cells causing the regression and inhibition of established tumor. Int J Cancer 1980;25:819–25.
40. Kershaw MH, Jackson JT, Haynes NM, Teng MW, Moeller M, Hayakawa Y, et al. Gene-engineered T cells as a superior adjuvant therapy for metastatic cancer. J Immunol 2004;173:2143–50.
41. Lotze MT, Zeh HJ, Rubartelli A, Sparvero LJ, Amoscato AA, Washburn NR, et al. The grateful dead: damage-associated molecular pattern molecules and reduction/oxidation regulate immunity. Immunol Rev 2007;220:60–81.
42. Peter C, Wesselborg S, Herrmann M, Lauber K. Dangerous attraction: phagocyte recruitment and danger signals of apoptotic and necrotic cells. Apoptosis 2010;15:1007–28.
43. Gough MJ, Crittenden MR, Sarff M, Pang P, Seung SK, Vetto JT, et al. Adjuvant therapy with agonistic antibodies to CD134 (OX40) increases local control after surgical or radiation therapy of cancer in mice. J Immunother 2010;33:798–809.
44. Palazon A, Teijeira A, Martinez-Forero I, Hervas-Stubbs S, Roncal C, Penuelas I, et al. Agonist anti-CD137 mAb act on tumor endothelial cells to enhance recruitment of activated T lymphocytes. Cancer Res 2011;71:801–11.